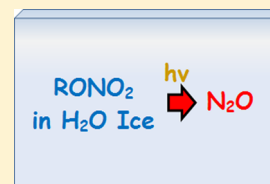


## Cold-Surface Photochemistry of Selected Organic Nitrates

Daniel O'Sullivan,<sup>\*,§</sup> Ryan P. McLaughlin,<sup>\*,‡</sup> Kevin C. Clemitshaw,<sup>||</sup> and John R. Sodeau<sup>\*,†</sup><sup>†</sup>Department of Chemistry, Centre for Research into Atmospheric Chemistry, University College, Cork, Ireland<sup>‡</sup>Department of Chemistry, Seattle University, 901 12th Avenue, Seattle, Washington 98122, United States<sup>||</sup>Department of Earth Sciences, Royal Holloway, University of London Egham, Surrey TW20 0EX, U.K.

**ABSTRACT:** Reflection–absorption infrared (RAIR) spectroscopy has been used to explore the low temperature condensed-phase photochemistry of atmospherically relevant organic nitrates for the first time. Three alkyl nitrates, methyl, isopropyl, and isobutyl nitrate together with a peroxyacyl nitrate, peroxyacetyl nitrate (PAN), were examined. For the alkyl nitrates, similar photolysis products were observed whether they were deposited neat to the gold substrate or codeposited with water. In addition to peaks associated with the formation of an aldehyde/ketone and NO, a peak near 2230 cm<sup>-1</sup> was found to emerge in the RAIR spectra upon UV photolysis of the thin films.

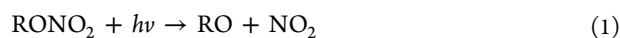
Together with evidence obtained by thermal programmed desorption (TPD), the peak is attributed to the formation of nitrous oxide, N<sub>2</sub>O, generated as a product during the photolysis. On the basis of the known gas-phase photochemistry for the alkyl nitrates, an intermediate pathway involving the formation of nitroxyl (HNO) is proposed to lead to the observed N<sub>2</sub>O photoproduct. For peroxyacetyl nitrate, CO<sub>2</sub> was observed as a predominant product upon photolytic decomposition. In addition, RAIR absorptions attributable to the formation of methyl nitrate were also found to appear upon photolysis. By analogy to the known gas-phase and matrix-isolated-phase photochemistry of PAN, the formation of methyl nitrate is shown to likely result from the combination of alkoxy radicals and nitrogen dioxide generated inside the thin films during photolysis.



## ■ INTRODUCTION

It is widely recognized that the oxides of nitrogen, NO and NO<sub>2</sub> (NO + NO<sub>2</sub> ≡ NO<sub>x</sub>), play critical roles in the chemistry of the lower atmosphere, participating in the production of ozone and modulating the lifetime of the hydroxyl radical.<sup>1</sup> Consequently, significant efforts have been devoted to characterizing the atmospheric fates of species that can act as precursors and sinks for NO<sub>x</sub>. Of particular interest to researchers examining the chemistry of remote regions have been organic nitrates, such as alkyl nitrates (RONO<sub>2</sub>) and peroxyacyl nitrates (RC(O)OONO<sub>2</sub>). Owing to their relative stability toward decomposition, these species can undergo long-range transport away from sources of pollution.<sup>2–4</sup> Upon decomposition, alkyl and peroxyacyl nitrates can produce reactive NO<sub>x</sub> in areas far removed from their formation. Given the importance of the organic nitrates as temporary NO<sub>x</sub> reservoirs, characterization of their photolysis pathways has been the subject of a substantial number of studies.<sup>2,3,5–8</sup> However, the potential role of ice surfaces in the photochemical processing of organonitrates has not yet been investigated, despite the fact that alkyl nitrates are thought to be a significant contributor to the total reactive nitrogen oxides (NO<sub>y</sub>) at the poles.<sup>9–12</sup>

In the troposphere, alkyl nitrates tend to be stable toward thermolysis<sup>5</sup> but are susceptible to gradual decomposition by photolysis and reaction with the hydroxyl radical.<sup>2,3</sup> To date, the photolysis pathways and UV absorption cross sections of several alkyl nitrates have been examined in the gas phase.<sup>3,6,7,13–16</sup> The main photodissociation channel for the alkyl nitrates is thought to be<sup>3,8,13–15</sup>



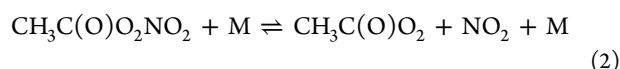
Talukdar et al. report the quantum yield of channel (1) approaches unity ( $\lambda = 248$  nm) for methyl nitrate,<sup>3</sup> whereas for the C<sub>3</sub>–C<sub>5</sub> alkyl nitrates, Zhu et al. have also found quantum yields of unity following photodissociation at 308 nm.<sup>16</sup>

At wavelengths above 240 nm, the UV absorption spectra of the alkyl nitrates are dominated by an n– $\pi^*$  transition, with absorption cross sections increasing with both the degree of substitution and carbon chain length.<sup>2,17</sup> Notably, however, the absorption cross sections trail off rapidly in the actinic region ( $\lambda > 290$  nm), limiting the rates of photolysis of the alkyl nitrates in the troposphere.<sup>2,3,6</sup> Estimated surface level lifetimes (due to both photolysis and reaction with hydroxyl radicals) at Northern midlatitudes vary from weeks during the winter to days during the summer.<sup>2</sup> Consequently, alkyl nitrates remain sufficiently long-lived to permit their long-range transport from sources and can impact upon tropospheric photochemistry in regions as remote as the poles.<sup>2,3</sup> For instance, in the Arctic, alkyl nitrates have been found to be substantial contributors to the NO<sub>y</sub> budget, comprising 10–20%,<sup>9,10</sup> whereas at the Antarctic alkyl nitrates have also been found to represent a major component of the total reactive nitrogen oxides.<sup>11,12</sup>

For peroxyacetyl nitrate (PAN), both gas-phase thermolysis and photolysis play important roles in its removal from the atmosphere, whereas reaction with hydroxyl radical is too slow to be of importance throughout the troposphere.<sup>4,5</sup> Thermolysis has been extensively detailed<sup>18–21</sup> and proceeds to yield acylperoxy radicals and nitrogen dioxide via

Received: July 1, 2014

Revised: September 17, 2014



The rate of removal of PAN by thermolysis is critically dependent on temperature. Under typical conditions found near ground level ( $T = 290$  K), the lifetime of PAN due to thermal dissociation is on the order of minutes to hours, whereas at temperatures representative of the upper troposphere, the lifetime is on the order of years ( $T = 250$  K).<sup>22</sup> The gas-phase photochemistry of PAN has also been examined in detail.<sup>23–26</sup> Although a wide variety of photoproducts are possible, the dominant decomposition channels for UV photolysis are<sup>23,25,26</sup>



Both photolysis channels are expected to have quite different outcomes in the atmosphere. Although the products of (3) can recombine to re-form PAN, the instability of the acetoxy product in pathway (4) leads to the irreversible loss of PAN and the release of  $\text{NO}_x$  following the photolysis of  $\text{NO}_3$ . Mazely and co-workers identified  $\text{NO}_2$  as the dominant photoproduct (quantum yield,  $\Phi_{\text{NO}_2} = 0.83 \pm 0.09$ ) following pulsed laser photolysis at 248 nm,<sup>25</sup> whereas the wavelength-dependent yield for  $\text{NO}_3$  has been found to vary from 0.19 to 0.41 across the wavelength region 248–308 nm.<sup>23,24,27</sup> However, the measured absorption cross sections for PAN<sup>4,28</sup> are sufficiently low that photolysis is not an important process at altitudes <7 km, where thermolysis dominates.<sup>4</sup> At low temperatures, PAN is stable enough to permit the transport of  $\text{NO}_x$  to remote regions of the globe, including the poles. Anomalously high contributions of PAN to  $\text{NO}_y$  have been observed at both poles, with  $[\text{PAN}]/[\text{NO}_y]$  reaching levels of up to 0.5–0.9 in the Arctic during springtime, as well as dominating the  $\text{NO}_y$  budget in the Antarctic.<sup>12,29,30</sup>

Past research has shown that heterogeneous transformations, taking place at the surface of ices, can play important roles in the atmospheric fates of important nitrogen oxides. However, despite the significance of the organic nitrates as sources of reactive nitrogen oxides at the poles, the heterogeneous photochemistry of these compounds in the presence of water ice has not been investigated to date. Here, by employing modern surface science techniques such as reflection–absorption infrared spectroscopy (RAIRS) in tandem with thermal programmed desorption (TPD) measurements, the condensed-phase photochemistry of three alkyl nitrates ( $R = \text{methyl, isopropyl, and isobutyl}$ ) and peroxyacetyl nitrate have been examined.

## ■ EXPERIMENTAL SECTION

Detailed descriptions of the experimental apparatus have been discussed elsewhere,<sup>31</sup> and therefore only a brief overview is presented here. Thin film samples were dosed onto a gold substrate contained within an ultrahigh vacuum (UHV) chamber. The chamber pressure was maintained at  $<10^{-8}$  mbar between experiments, and the gold foil was routinely cleaned between measurements by heating to 500 K. FTIR spectra collected in the reflection absorption mode were collected using a Bruker Vertex 70 FTIR spectrometer equipped with a liquid-nitrogen-cooled HgCdTe detector. Spectra were collected at a resolution of  $2 \text{ cm}^{-1}$ . The UHV chamber was also fitted with a quadrupole mass spectrometer

(EPIC 300, Hiden Analytical) to analyze gas-phase products released from the thin films, using electron impact ionization with 70 eV ionization potential. Thermal programmed desorption (TPD) measurements were conducted at a ramp rate of  $0.8 \text{ K s}^{-1}$ . Photolysis experiments were conducted using an unfiltered broadband Xe arc lamp source (Oriel, model 60010,  $\lambda > 230 \text{ nm}$ ), with the samples exposed through a quartz window on the side of the chamber. Dosing of the vapors onto the cold substrate ( $T_{\text{initial}} \sim 113 \text{ K}$ ) was conducted by means of either manually operated valves or piezoelectric pulsed valves. Estimating the number of monolayers from the exposure time and pressure ( $10^{-6} \text{ Torr s} = 1 \text{ Langmuir} \approx 1 \text{ monolayers}$ )<sup>32</sup> leads to an average of approximately 100 monolayers for the experiments performed in this study. In codeposition experiments, dosing was performed such that there was an excess of the organic nitrate relative to water introduced to the chamber (alkyl/peroxyacetyl nitrate:water  $\approx 3:1$ ). All samples were degassed using three freeze–pump–thaw cycles on a vacuum line prior to dosing into the UHV chamber. The duration of each photolysis experiment was primarily limited by the length of time the HgCdTe detector could be held at temperatures low enough to permit spectral acquisition. The ability to maintain the detector at sufficiently low temperatures by refilling with liquid nitrogen deteriorated throughout the course of an experiment, due to the condensation of water ice in the cooling reservoir of the detector. With this constraint in mind, the RAIR spectra indicated below have been selected to highlight the largest spectral changes that were observed during the course of photolysis experiments.

Samples of isopropyl nitrate (99%) and isobutyl nitrate (95%) were purchased from Sigma and used without further purification. Methyl nitrate was prepared via the low temperature nitration of methanol, as described by Clemitshaw et al.<sup>2</sup> Nitrogen gas was bubbled through a stirred mixture of 10 mL of 99.5% nitric acid and 10 mL of 98% sulfuric acid held at  $0^\circ\text{C}$ , before and during the slow dropwise addition of 7 mL of methanol. The alkyl nitrate product was separated and washed with Milli-Q purified water and then dried with anhydrous magnesium sulfate. After the removal of water, the methyl nitrate was filtered into a test tube that was stoppered and stored in a dark freezer at  $-15^\circ\text{C}$ .

Peroxyacetyl nitrate (PAN) was synthesized by the low-temperature nitration of peroxyacetic acid as described by Nikitas et al.<sup>33</sup> Nitrogen gas was bubbled through a stirred solution containing 3.3 mL of peroxyacetic acid and 2.6 mL of 98% sulfuric acid dissolved in 40 mL of tridecane held at  $0^\circ\text{C}$  in an ice bath for 5 min before, during, and for 10 min after the dropwise addition of 0.7 mL of 99.5% nitric acid. To remove unreacted acids after the nitration step, the PAN product (in the tridecane solvent) was washed with Milli-Q purified water held at  $0^\circ\text{C}$ . After the product was dried by adding anhydrous magnesium sulfate, the PAN solution was filtered into a test tube, which was stoppered and stored in a dark freezer at  $-15^\circ\text{C}$ .

## ■ RESULTS

**Methyl Nitrate.** The RAIR spectra of methyl nitrate,  $\text{MeONO}_2$ , both deposited neat to the gold substrate and codeposited with water, are illustrated in Figure 1. The spectral assignments are presented in Table 1, where previous values obtained from the literature are also listed for comparison.

A number of features characteristic of the alkyl nitrates are immediately evident in the RAIR spectrum of methyl nitrate

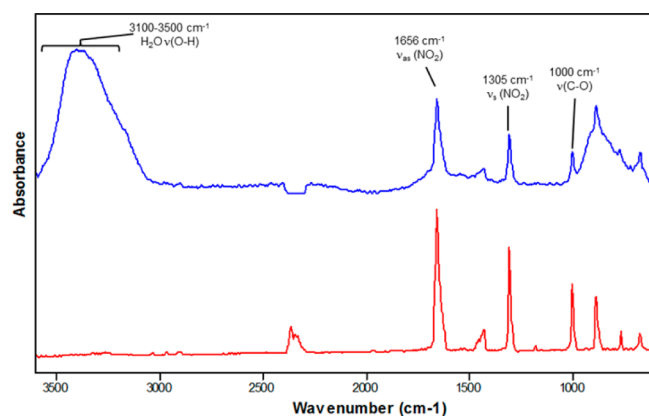


**Figure 1.** RAIR spectrum of methyl nitrate deposited neat (red trace) and codeposited with water (blue trace) at 113 K.

**Table 1.** RAIR Normal Mode Assignments for a Thin Methyl Nitrate Film Co-deposited with Water<sup>a</sup>

mode	description	matrix isolated <sup>34</sup>	liquid <sup>35</sup>	RAIRS
		10 K, N <sub>2</sub> , MR = 50:1	298 K	113 K, codep H <sub>2</sub> O
$\nu_1$	$\nu(\text{C-H})$	2965 w	3040 mw	3030
$\nu_2$	$\nu(\text{C-H})$	2930 w	2963 m	2964
$\nu_3$	$\nu_{\text{as}}(\text{NO}_2)$	1652 vs	1634 vs	1656 (1658)
$\nu_4$	$\delta(\text{CH}_3)$	1465 w	1458 mw	1454
$\nu_5$	$\delta(\text{CH}_3)$	1435 w	1429 m	1425
$\nu_6$	$\nu_{\text{s}}(\text{NO}_2)$	1293 vs	1282 vs	1305 (1307)
$\nu_7$	$\rho(\text{CH}_3)$	1177 w	1174 mw	1179
$\nu_8$	$\nu(\text{C-O})$	1004 s	993 s	1000
$\nu_9$	$\nu(\text{N-O})$	860 m	859 s	884
$\nu_{16}$	$\rho(\text{NO}_2)$	760 w	759 ms	765

<sup>a</sup>Wavenumbers in brackets are those found for the neat thin films and are listed when they differ from those of the co-deposited films.

codeposited with water. The most intense band arising from the presence of MeONO<sub>2</sub> is evident at 1656 cm<sup>-1</sup> and is due to the asymmetric NO<sub>2</sub> stretching vibration.<sup>34,35</sup> Similarly, the symmetric NO<sub>2</sub> stretching vibration is found to absorb at 1305 cm<sup>-1</sup>. The C–O stretching vibration, also common to all alkyl nitrates, is located in the RAIR spectrum at 1000 cm<sup>-1</sup>. A number of features characteristic of the methyl group are also evident in the spectrum, the most intense of which is the CH<sub>3</sub> deformation, centered at 1425 cm<sup>-1</sup>. The methyl nitrate peak positions for both the codeposited and neat thin films were found to change little, with the largest spectral shift observed being a small red-shifting ( $\Delta\tilde{\nu} = -2$  cm<sup>-1</sup>) of the NO<sub>2</sub>-stretching modes in the codeposited thin film relative to the spectra of the neatly deposited films.

Upon irradiation of the samples with the broadband source, features assigned to MeONO<sub>2</sub> were observed to slowly drop in intensity, while a number of new peaks emerged. In Figure 2, RAIR difference spectra of a codeposited thin film are presented to illustrate the spectral changes resulting from photolysis over the course of 3 h. These difference spectra were obtained by subtraction of the spectra obtained prior to irradiation (Figure 1), from those obtained at a given time throughout the photolysis period. Consequently, increasing peaks indicate the formation of new species, whereas decreasing peaks indicate loss.

Within the first hour of photolysis, bands assigned to MeONO<sub>2</sub> were observed to drop in intensity, while a new IR band at 1716 cm<sup>-1</sup> grew in. The appearance of this peak, which

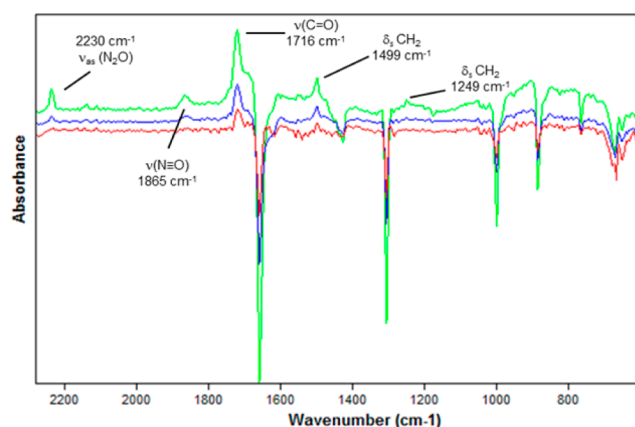


**Figure 2.** RAIR difference spectrum illustrating the changes observed upon photolysis of a thin methyl nitrate film that was codeposited with water. Shown are the difference spectra after 1 h (red trace), 2 h (blue trace), and 3 h (green trace).

is characteristic of a carbonyl stretching vibration,<sup>36</sup> is also accompanied by the development of bands at 1499 and 1249 cm<sup>-1</sup>, which grow at similar rates. Together, these three bands were found to correspond well with transmission IR features previously reported for solid formaldehyde.<sup>37</sup> Two further weak features not attributable to formaldehyde were also present at 1865 and 2230 cm<sup>-1</sup>. The former peak is readily identifiable as the N–O stretching vibration of nitric oxide, NO.<sup>38</sup> Notably, the latter band at 2230 cm<sup>-1</sup> has previously been found to arise due to a photolysis product in low temperature RAIR spectra of primary and tertiary alkyl nitrites (RONO), where it was shown to result from the asymmetric stretch of nitrous oxide, N<sub>2</sub>O.<sup>39</sup>

**Isopropyl Nitrate.** The RAIR spectra of isopropyl nitrate, both deposited neat to the gold substrate and codeposited with water, are presented in Figure 3. The bands observed in the RAIR spectra are assigned in Table 2, where vibrational wavenumbers from the IR spectrum of the neat liquid<sup>40</sup> are also listed for comparison.

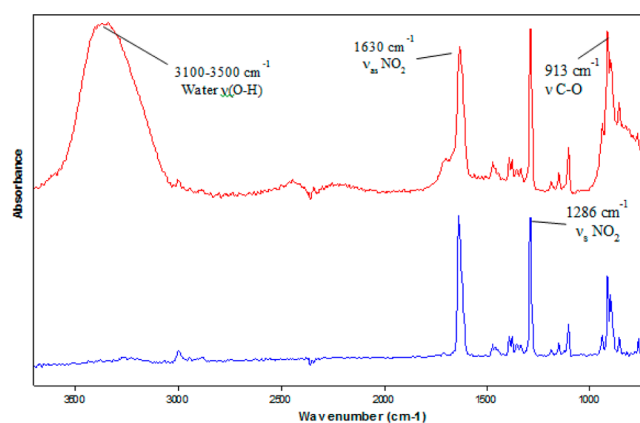


**Figure 3.** RAIR spectra of isopropyl nitrate deposited neat (red trace) and codeposited with water (blue trace).

Whether deposited neat or codeposited with water, the main RAIR band positions of isopropyl nitrate were found to be similar. The largest spectral shift observed upon codeposition was a small red-shifting ( $\Delta\tilde{\nu} = -4$  cm<sup>-1</sup>) of the NO<sub>2</sub> stretching modes relative to the spectra of the neatly deposited films. More significant shifts in vibrational wavenumbers can be seen

**Table 2. Assignments of RAIR Wavenumbers ( $\text{cm}^{-1}$ ) Observed for Isopropyl Nitrate Co-deposited with Water<sup>a</sup>**

assignment	liquid <sup>40</sup>	RAIR
	298 K	113 K, codep H <sub>2</sub> O
$\nu_{\text{as}}(\text{CH}_3)$	2993 mw	2993
$\nu(\text{C-H})$	2944 w	2946
$\nu_{\text{as}}(\text{CH}_3)$	2903 w	2906
$\nu_{\text{as}}(\text{NO}_2)$	1627 vs	1630 (1634)
$\delta(\text{CH}_3)$	1471 w	1472
$\delta(\text{CH}_3)$	1457 w	1457
$\delta(\text{CH}_3)$	1446 w	1444
$\nu_{\text{s}}(\text{C-C-C})$	1390 mw	1389
$\nu_{\text{as}}(\text{C-C-C})$	1378 mw	1376
$\rho(\text{C-C-C})$	1351 w	1350
$\rho(\text{C-C-C})$	1332 w	1333
$\nu_{\text{s}}(\text{NO}_2)$	1282 s	1286 (1290)
C-C-C wag	1183 w	1185
$\nu(\text{C-C})$	1145 w	1149
$\nu_{\text{as}}(\text{C-C})$	1124 w	1124
C-C-C wag	1103 m	1104
$\delta(\text{CH}_3)$	937 w	937
$\nu(\text{C-O})$	910 m	913
$\nu(\text{N})-\text{O}$	881 s	896
$\rho(\text{NO}_2)$	853 m	854

<sup>a</sup>Wavenumbers in brackets are those found for a neat thin film and are listed when they varied from those found for the co-deposited thin films.

when the RAIR spectrum of isopropyl nitrate was codeposited with water as compared with the analogous spectrum obtained for methyl nitrate shown in Figure 1. Relative to methyl nitrate, the  $\nu_{\text{as}}(\text{NO}_2)$  mode of isopropyl nitrate is red-shifted by  $\Delta\tilde{\nu} = -26 \text{ cm}^{-1}$ , while a similar change of  $\Delta\tilde{\nu} = -19 \text{ cm}^{-1}$  is apparent by comparison to the  $\nu_{\text{s}}(\text{NO}_2)$  modes. The linking C-O stretch absorbs at  $913 \text{ cm}^{-1}$ , which is significantly red-shifted in frequency ( $\Delta\tilde{\nu} = -87 \text{ cm}^{-1}$ ) relative to that observed for the methyl analogue (Table 1). In addition to bands attributable to the nitric ester functionality (R-ONO<sub>2</sub>), features representative of an alkyl moiety are present in the RAIR spectra. Consistent with the increased complexity of the alkyl group, vibrational modes not seen in the RAIR spectra of MeONO<sub>2</sub> are present for its isopropyl analogue. Such a feature is apparent in the 1300–1400  $\text{cm}^{-1}$  region of the isopropyl nitrate RAIR spectrum, where new vibrations arise due to C-C-C stretching and rocking modes.

Upon photolysis of the thin films of isopropyl nitrate, either deposited neat or codeposited with water, bands associated with the parent organic nitrate are observed to lose intensity in the RAIR difference spectra (Figure 4). Concurrently, a positive band at  $1705 \text{ cm}^{-1}$  develops, which is attributable to a C=O stretching vibration of an aldehyde or ketone.<sup>40</sup> The appearance of this band is also accompanied by the development of weaker peaks at 1425, 1368, and  $1242 \text{ cm}^{-1}$ , which grow at a similar rate. Together, these emerging bands are found to correspond well with RAIR vibrational wavenumbers previously reported for propanone deposited to water ice films at 95 K.<sup>41</sup> Similar to what was observed in the RAIR spectra during the photolysis of methyl nitrate (Figure 2), a further weak band at  $2230 \text{ cm}^{-1}$  was found to appear upon photolysis of the thin films, identifiable as the asymmetric stretching vibration of nitrous oxide.<sup>39,42</sup> The presence of N<sub>2</sub>O within the thin films after photolysis was further probed using TPD measurements, as

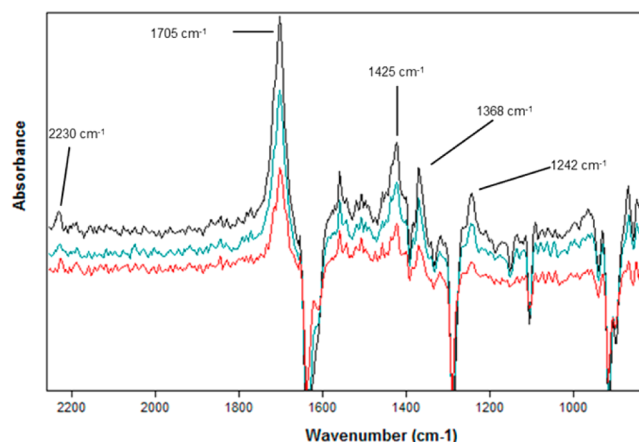


**Figure 4.** RAIR difference spectra of a thin film of isopropyl nitrate, codeposited with water. Shown are the spectra taken after photolysis for 40 min (red trace), 80 min (green trace), and 120 min (black trace).

shown in Figure 5. Here, the initial desorption of a volatile species with  $m/z = 44$ , 28, and 16 can be seen, consistent with

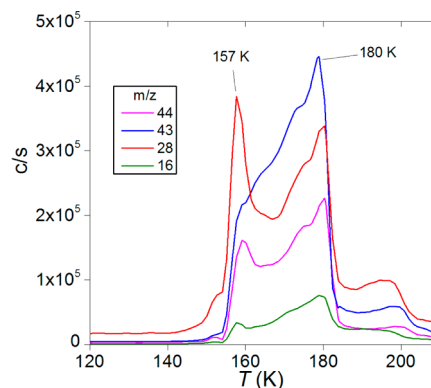


**Figure 5.** TPD profile obtained from a codeposited isopropyl nitrate/H<sub>2</sub>O film subjected to 2 h of photolysis. Observed are fragments associated with N<sub>2</sub>O (N<sub>2</sub>O<sup>+</sup>,  $m/z = 44$ ; N<sub>2</sub><sup>+</sup>,  $m/z = 28$ , O<sup>+</sup>,  $m/z = 16$ ) and a fragment associated with isopropyl nitrate and propanone (CH<sub>3</sub>CO<sup>+</sup>,  $m/z = 43$ ).

the loss of N<sub>2</sub>O from the films.<sup>43</sup> Notably, the desorption of these fragments peaks at two distinct temperatures (157 and 180 K), similar to what has been reported when water ice is codeposited with other volatile species, such as CO<sub>2</sub>.<sup>44</sup> The initial desorption peaking at 157 K can be explained on the basis of a “volcano” desorption as described by Smith et al.,<sup>45</sup> where volatile species trapped in a water ice matrix are released during the formation of connected desorption pathways as amorphous solid water converts to crystalline ice. Subsequently, the remaining trapped volatile species are then released during the desorption of water ice at 180 K.

**Isobutyl Nitrate.** The RAIR spectra of isobutyl nitrate, both deposited neat and codeposited with water, are presented in Figure 6. In each case, the spectra were recorded directly after deposition at 113 K. The wavenumbers of the RAIR band centers are assigned in Table 3, where previous literature values obtained from IR spectra of the neat liquid<sup>40</sup> are listed for comparison.

Apart from a small red-shifting of  $\nu_{\text{as}}(\text{NO}_2)$  mode by  $5 \text{ cm}^{-1}$ , the presence of water had little effect on the positions of the

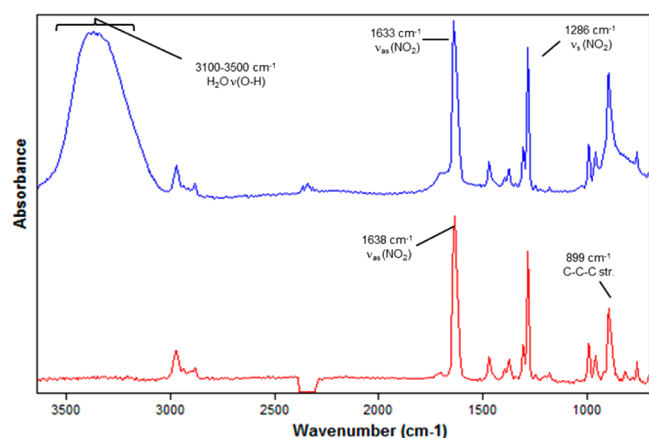


**Figure 6.** RAIR spectra of isobutyl nitrate deposited neat (red trace) and codeposited with water (blue trace). Both spectra were recorded directly after deposition at 113 K.

**Table 3. Assignments of RAIR Features Observed for Isobutyl Nitrate Co-deposited with Water<sup>a</sup>**

description	liquid <sup>140</sup>	RAIR
	298 K, neat	113 K, codep H <sub>2</sub> O
$\nu_{as}(\text{CH}_3)$	2973 m	2969
$\nu_{as}(\text{CH}_3)$	2940 w	2936
$\nu_s(\text{CH}_3)$	2880 m	2878
$\nu_{as}(\text{NO}_2)$	1630 vs	1633 (1638)
$\delta(\text{CH}_3)$	1472 m	1472
$\delta(\text{CH}_3)$	1438 w	1450
$\nu_s(\text{C}-\text{C}-\text{C})$	1395 m	1393
$\nu_{as}(\text{C}-\text{C}-\text{C})$	1373 m	1377
CH <sub>2</sub> wag	1356 m	
$\nu_s(\text{C}-\text{C})$	1305 m	1304
$\nu_s(\text{NO}_2)$	1281 s	1286 (1289)
CH <sub>2</sub> rock	1249 w	1246
C-C-C wag	1180 w	1181
$\nu(\text{C}-\text{O})$	990 m	989
$\nu(\text{C}-\text{C})$	962 m	960
$\delta(\text{C}-\text{C}-\text{C})$	893 m	896
$\nu(\text{N}-\text{O})$	875 m	
$\rho(\text{NO}_2)$	856 m	852

<sup>a</sup>Wavenumbers in brackets are those found for a neat thin film, and are listed when they varied from those found for the co-deposited thin films.

RAIR peak maxima. In addition to the intense RAIR band due to the  $\nu_{as}(\text{NO}_2)$  mode, further absorptions originating from the presence of the nitrate functionality are again identifiable in the spectra. The NO<sub>2</sub> symmetric stretching, rocking, and wagging vibrations are all found to be within  $\sim 5 \text{ cm}^{-1}$  of the analogous absorptions observed for isopropyl nitrate, as shown in Table 2. By contrast, the  $\nu(\text{C}-\text{O})$  mode of the nitric ester, which is centered at  $989 \text{ cm}^{-1}$  for isobutyl nitrate, lies much closer to that found for methyl nitrate ( $1000 \text{ cm}^{-1}$ ) than was observed for isopropyl nitrate ( $913 \text{ cm}^{-1}$ ).

Upon photolysis, the RAIR difference spectrum shown in Figure 7 indicates that the behavior of isobutyl nitrate mirrors that previously seen for both the methyl and isopropyl nitrates. At  $2230 \text{ cm}^{-1}$ , an absorption assigned to N<sub>2</sub>O is again found to grow as the thin films are photolyzed. Notably, this photolysis behavior mimics that found previously for the corresponding alkyl nitrite (RONO, where R = *i*-But),<sup>39</sup> where an identical

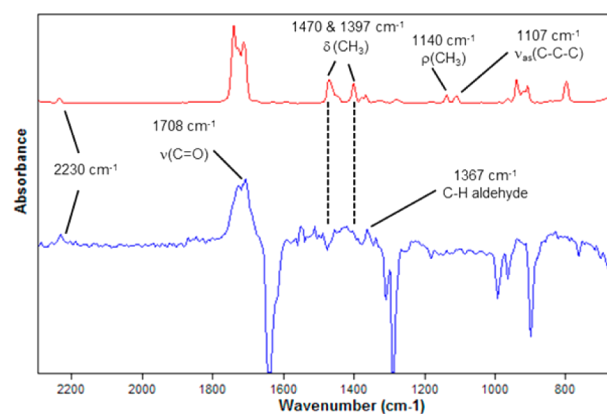


**Figure 7.** RAIR difference spectrum of a codeposited water/isobutyl nitrate thin film, which was photolyzed for 3.5 h (blue trace). Also shown is the RAIR spectrum of 2-methylpropanal codeposited with N<sub>2</sub>O at 113 K for comparison (red trace), which has been scaled down by a factor of 5 for comparison.

band in the RAIR spectra due to N<sub>2</sub>O also developed upon irradiation ( $\lambda > 230 \text{ nm}$ ). A positive band at  $1708 \text{ cm}^{-1}$  also develops during photolysis, indicating the formation of an aldehyde or ketone.<sup>36</sup> By analogy to methyl and isopropyl nitrate, this absorption is most likely to arise from the formation of 2-methylpropanal (isobutanal). However, the major hydrocarbon modes of this aldehyde were difficult to discern from the difference spectra. A comparison between the RAIR spectrum of 2-methylpropanal codeposited with N<sub>2</sub>O with the RAIR difference spectra taken during photolysis provides an explanation for the apparent absence of further hydrocarbon modes. As indicated in Figure 7, intense RAIR features of the deposited aldehyde (e.g., the CH<sub>3</sub> deformation modes at  $1470$  and  $1397 \text{ cm}^{-1}$ ) coincide with those of isobutyl nitrate. Furthermore, the remaining absorption features of 2-methylpropanal that do not overlap with peaks from isobutyl nitrate (e.g.,  $1140$  and  $1107 \text{ cm}^{-1}$ ) are weak and therefore become lost within the noise of the difference spectra. Table 4 shows a comparison of absorption features present in the transmission IR spectrum of 2-methylpropanal with those observed in the current RAIR study.

In Figure 8, the relative loss rates of the three alkyl nitrates codeposited with water are compared using the decrease in intensity from the  $\nu_{as}(\text{NO}_2)$  peak for each. The loss rates on photolysis were found to follow the trend methyl < isobutyl < isopropyl, which is the same trend found for the UV absorption

**Table 4. Comparison of Absorption Features Present in the Transmission IR Spectrum of 2-Methylpropanal with Those Observed in the Current Study<sup>a</sup>**

mode	description	solid <sup>146</sup>	RAIR
		neat, 90 K	photoproduct, 113 K
$\nu_6$	$\nu(\text{C}=\text{O})$	1707	1708
$\nu_{23}$	$\delta_{as}(\text{CH}_3)$	1477	<i>a</i>
$\nu_9$	$\delta_s(\text{CH}_3)$	1397	<i>a</i>
$\nu_{10}$	aldehydic (C-H)	1367	1367
$\nu_{26}$	$\alpha$ CH bend	1273	<i>a</i>
$\nu_{13}$	$\rho(\text{CH}_3)$	1138	
$\nu_{27}$	$\nu_{as}(\text{C}-\text{C}-\text{C})$	1107	

<sup>a</sup>The peak coincides with an absorption of isobutyl nitrate and was therefore not observable in the current study.

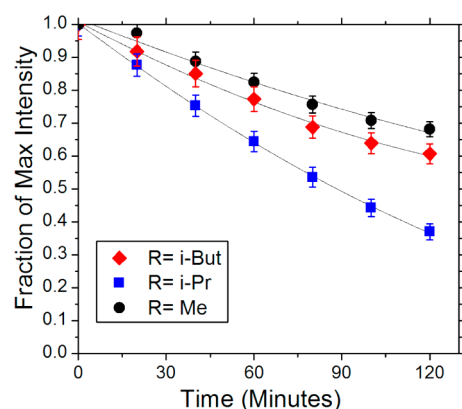


**Figure 8.** Normalized intensity of the  $\nu_{as}(\text{NO}_2)$  absorption peaks versus photolysis time for the three alkyl nitrates investigated during this study. The intensities were determined from RAIR spectra of the alkyl nitrates codeposited with water.

cross sections for these alkyl nitrates in the gas and liquid phase.<sup>2,6,17</sup>

**Peroxyacetyl Nitrate (PAN).** In Figure 9, the RAIR spectra of peroxyacetyl nitrate (PAN), deposited neat and codeposited

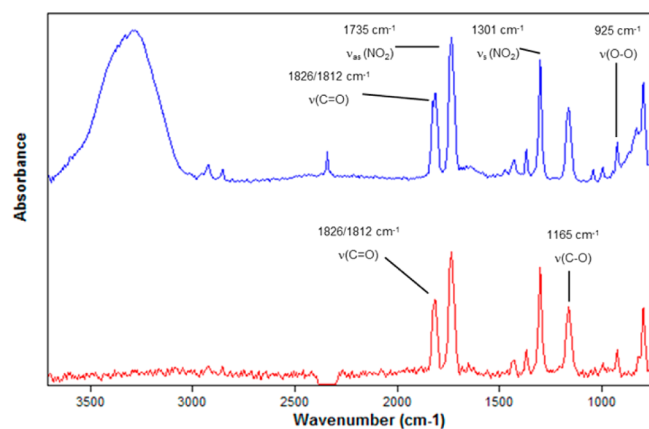


**Figure 9.** RAIR spectra of peroxyacetyl nitrate, deposited neat to the gold substrate at 113 K (red trace) and codeposited with water (blue trace).

with water, are illustrated. In each case, the spectra were recorded directly after deposition to the gold substrate at 113 K. Assignments of the RAIR spectral features are presented in Table 5, together with IR absorption wavenumbers from the literature for comparison.

The RAIR spectra obtained for the neatly deposited PAN films were found to be similar to spectra for when it had been codeposited with water. In both spectra, the  $\nu(\text{C}=\text{O})$  stretching mode was found to split into two bands at 1826 and 1812  $\text{cm}^{-1}$ , with the splitting being more pronounced in the codeposited films, and the 1826  $\text{cm}^{-1}$  peak only appearing as a shoulder when films were deposited neat. When these are compared to previous gas-phase IR spectra of PAN,<sup>47</sup> both red and blue shifts of vibrational absorptions in the solid become apparent. The largest difference of IR absorption wavenumbers between the two phases occurs for the  $\nu(\text{C}=\text{O})$  mode, with  $\Delta\tilde{\nu} > -16 \text{ cm}^{-1}$  in the solid relative to the gas phase.

Upon photolysis of the codeposited thin film, the intensity of peaks due to the peroxyacetyl nitrate were observed to decrease. The largest spectral change observed during the photolysis was

**Table 5.** Assignments of the Vibrational RAIR Bands Observed for Peroxyacetyl Nitrate, Together with Literature Values for Comparison<sup>a</sup>

mode	description	gas <sup>47</sup>	matrix <sup>47</sup>	RAIR
			Ar, 10 K, M.R.= 500:1	113 K, codep. with water
$\nu_4$	$\nu(\text{C}=\text{O})$	1842 s	1835 s	1812 (1826)
$\nu_5$	$\nu_{as}(\text{NO}_2)$	1741 vs	1731 vs	1735
$\nu_{6-8}$	$\sigma_{as}(\text{CH}_3)$	1430 w	1435 w	1430
	$\sigma_s(\text{CH}_3)$	1371 m	1368 m	1368
$\nu_9$	$\nu_s(\text{NO}_2)$	1302 s	1300 s	1301
$\nu_{10}$	$\nu(\text{C}-\text{O})$	1162 s	1154 s	1165
$\nu_{11,12}$	$\rho(\text{CH}_3)$	1055 w	1043 w	1041
$\nu_{13}$	$\nu(\text{C}-\text{C})$	990 m	988 m	995
$\nu_{14}$	$\nu(\text{O}-\text{O})$	930 m	927 m	925
$\nu_{15}$	$\nu(\text{N}-\text{O})$	821 m	821 m	828
$\nu_{16}$	$\sigma(\text{NO}_2)$	792 s	789 s	799

<sup>a</sup>Wavenumbers in brackets are those found for the neat thin film and are listed when they varied from those found for the co-deposited thin film.

the growth of an absorption peak at 2344  $\text{cm}^{-1}$ , which could be accounted for by the generation of carbon dioxide within the thin films (Figure 10).<sup>44</sup> No peaks associated with the RAIR

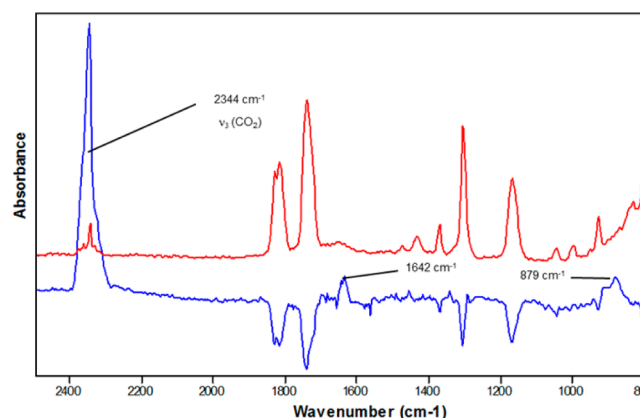


**Figure 10.** RAIR difference spectra of a thin film of PAN, codeposited with water. Shown is the difference spectrum recorded after 4 h of photolysis (red trace). Also shown is the RAIR spectrum of the codeposited thin film prior to photolysis for comparison (blue trace).

spectrum of either NO or  $\text{NO}_2$ <sup>38</sup> were observed to form during photolysis. However, minor bands at 1642 and 879  $\text{cm}^{-1}$  were found to increase as a function of photolysis time. Notably, the only strong absorptions of methyl nitrate that do not overlap with those of PAN are found in these regions (Table 1). The apparent formation of carbon dioxide and methyl nitrate as photoproducts compares well with previous matrix isolation studies of PAN, where the same photolysis products have been reported upon irradiation at wavelengths below 300 nm.<sup>47</sup> The decrease with time of PAN due to photolysis, along with the concurrent formation of the peak at 1642  $\text{cm}^{-1}$  is depicted in Figure 11.

Further evidence for the generation of  $\text{MeONO}_2$  within the thin films was obtained from TPD measurements performed subsequent to photolysis of the codeposited thin films (Figure 12). For both methyl nitrate and PAN, the parent molecular ions are not observed in the (electron impact) mass spectra at energies between 20 and 70 eV.<sup>5,48</sup> Furthermore, the only

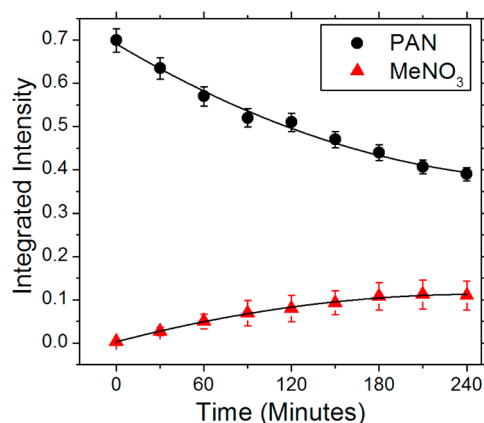


**Figure 11.** Loss rate of peroxyacetyl nitrate (PAN) from the thin films codeposited with water as tracked by the decrease of its  $\nu(\text{NO}_2)_s$  vibrational adsorption centered at  $1301\text{ cm}^{-1}$ . Also shown is the growth rate for the  $\nu(\text{NO}_2)_{as}$  peak of methyl nitrate at  $1642\text{ cm}^{-1}$ .

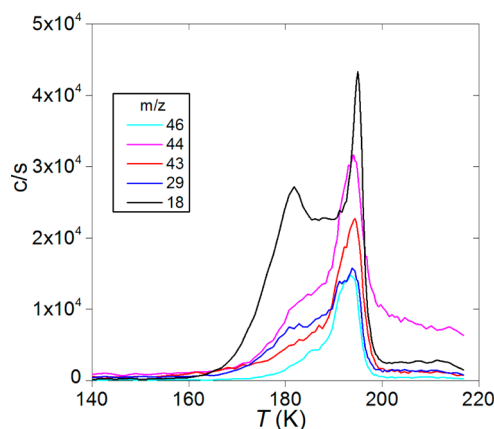


**Figure 12.** Thermal desorption profile of a thin film of PAN codeposited with water subsequent to photolysis. Shown are the major fragments associated with PAN ( $m/z = 43$ ,  $\text{CH}_3\text{CO}^+$ ;  $m/z = 44$ ,  $\text{CO}_2^+$ ;  $m/z = 46$ ,  $\text{NO}_2^+$ ),  $\text{MeONO}_2$  ( $m/z = 29$ ,  $\text{CHO}^+$ ), and  $\text{H}_2\text{O}$  ( $m/z = 18$ ,  $\text{H}_2\text{O}^+$ ). The trace for water ( $m/z = 18$ ) has been scaled down by a factor of 5 for comparison.

fragment of methyl nitrate that has not been documented to occur at the same mass to charge ratio for PAN is found at  $m/z = 29$  ( $\text{CHO}^+$ ).<sup>5,48–50</sup> The desorption of PAN was monitored via the generation of  $\text{CH}_3\text{CO}^+$  and  $\text{CO}_2^+$  fragments ( $m/z = 43$  and  $44$ , respectively).<sup>5,48</sup> Consistent with previous TPD measurements of pure water films deposited at low temperatures,<sup>51</sup> water ( $\text{H}_2\text{O}^+$   $m/z = 18$ ) begins to desorb from substrate at temperatures above 160 K. As the temperature is raised further, ions attributable to PAN ( $\text{CH}_3\text{CO}^+$ ,  $m/z = 43$ ;  $\text{CO}_2^+$ ,  $m/z = 44$ ) and methyl nitrate ( $\text{CHO}^+$ ,  $m/z = 29$ ) continue to be lost from the surface until around 200 K, where desorption ends.

## DISCUSSION

**Methyl, Isopropyl, and Isobutyl Nitrates.** In the current study, the solid-phase IR spectra of some simple alkyl nitrates ( $R = \text{Me}$ ,  $i\text{-Pr}$ ,  $i\text{-But}$ ), deposited both neat and codeposited with water have been reported for the first time. In general, the spectra obtained were quite similar to those previously reported for the liquid phase,<sup>40,52</sup> with only minor frequency shifts observed for the neatly deposited thin films. Additionally, when

the alkyl nitrates were codeposited with water onto the gold substrate, few spectral shifts or changes in relative intensity were observed in comparison with when deposited neat. One exception to this was the  $\nu_{as}(\text{NO}_2)$  mode of the alkyl nitrates, which was seen to red shift by up to  $5\text{ cm}^{-1}$  for the alkyl nitrates when codeposited with water. This red-shifting of the vibrational frequency can be accounted for by intermolecular interactions between water and the alkyl nitrates, which slightly decreases the  $\text{N}=\text{O}$  bond strength of the latter. Hydrogen bonding interactions, where the  $\text{N}=\text{O}$  group acts as an electron density donor, and the  $\text{H}-\text{O}$  group of water the acceptor provide a plausible explanation for this observation.

A number of spectral shifts also become apparent when the different alkyl nitrates were compared to one another. For instance, in the case of the  $\nu_{as}(\text{NO}_2)$  stretching vibration, it can be seen that for each additional methyl group attached to the  $\alpha$ -carbon of the alkyl nitrate, the vibrational frequency is progressively red-shifted. This trend has previously been observed for the liquid phase by Urbanski,<sup>52</sup> who attributed it to the accumulative inductive effect of increasing the alkyl substitution on the  $\alpha$ -carbon. Accordingly, for each additional alkyl group the  $\text{N}=\text{O}$  bond strength is decreased due to the decreasing positive character of the nitrogen atom.

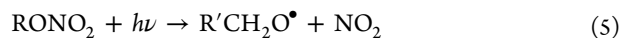
A dramatic reduction in the frequency ( $\Delta\tilde{\nu} = -87\text{ cm}^{-1}$ ) of the linking  $\text{C}-\text{O}$  stretching mode for isopropyl nitrate was observed, relative to the methyl and isobutyl nitrates. In the liquid phase, the region where this vibration occurs for all other  $\text{C}_1\text{-C}_5$  alkyl nitrates is around  $990\text{ cm}^{-1}$ .<sup>52</sup> However, for isopropyl nitrate, the region between  $1080$  and  $940\text{ cm}^{-1}$  is completely featureless, both in the RAIR spectra of the present study (Figure 3) and in previous liquid-phase FTIR spectra.<sup>40,52</sup> Although earlier researchers have simply left this mode unassigned,<sup>52</sup> McLaughlin et al. attributed a medium intensity absorption at  $910\text{ cm}^{-1}$  to the above stretching vibration.<sup>40</sup> The shifting of this band may be related to the unusual conformation that isopropyl nitrate adopts in the liquid phase. By contrast with the other alkyl nitrates, the plane in which the  $\text{NO}_3$  group lies is thought to be twisted away from the linking  $\text{C}-\text{O}$  bond axis in isopropyl nitrate.<sup>40</sup> As a result, the  $\text{C}-\text{O}$  bond itself may become strained, leading to the observed red-shift in vibrational frequency.

For all three of the alkyl nitrates, little information on their orientation within the thin films could be discerned from the RAIR measurements. Given the low symmetry of each of these species in the liquid phase ( $C_s$  for  $R = \text{Me}$ ,  $i\text{-But}$  and  $C_1$  for  $R = i\text{-Pr}$ )<sup>34,40</sup> the observed invariance of the RAIR absorption intensities with respect to the liquid-phase IR spectra may be expected. If, for example, the mirror planes of methyl and isobutyl nitrate are lost in the solid phase, the point group is reduced to the only subgroup of  $C_s$ , which is the trivial group  $C_1$ . In such a case the metal surface selection rule (MSSR), which leads to the loss of absorptions with vibrational transition dipole moments parallel to the surface,<sup>53</sup> cannot stimulate intensity changes of one vibration with respect to another. Conversely, if the parent alkyl nitrate retains  $C_s$  symmetry, but the solid phase is not highly ordered, no changes in the absorption intensities will be apparent. Hence, in the current study, RAIR spectra cannot distinguish between these two potential scenarios.

During the current investigation, the photolysis of all three alkyl nitrates proceeded in a similar fashion, leading to the formation of an aldehyde or ketone, along with a minor band at  $2230\text{ cm}^{-1}$ , characteristic of nitrous oxide.<sup>39,42</sup> For neatly

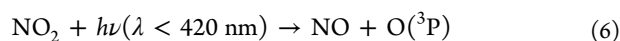
deposited thin films, a weak broad feature in the region 3100–3500  $\text{cm}^{-1}$  was also observed to emerge during photolysis experiments, consistent with the increasing presence of water ice. It should be noted that it is unclear whether the growth of peaks due to water ice in the neat thin films stemmed from photolysis products or the condensation of trace amounts of vapor in the UHV chamber during the course of an experiment. Regardless of this, the observation of peaks due to nitrous oxide together with those of an aldehyde or ketone in neatly deposited thin films suggests that the formation of products was insensitive to the relative excess of the organic nitrate over water. The loss rate of the three alkyl nitrates upon photolysis was found to proceed in the order  $R = \text{methyl} < \text{isobutyl} < \text{isopropyl}$ , which mirrors the trend found for the magnitude of the absorption cross sections in the gas<sup>2,6</sup> and liquid phases.<sup>17</sup> This increase in UV cross sections with increasing degree of substitution and carbon number has previously been shown by Csizmadia et al.<sup>17</sup> and Roberts et al.<sup>6</sup> to result from a combination of both structural and electronic effects caused by the alkyl substituents.

Past studies into the photolysis of alkyl nitrates have focused almost exclusively on determining the quantum yields for the primary processes.<sup>3,7,16</sup> Indeed, by analogy to the known gas-phase photolysis pathways for the alkyl nitrates,<sup>2,3,5,6</sup> dissociation of the weak O–N bond is also likely to take place under the conditions employed in the current study:

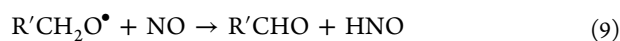
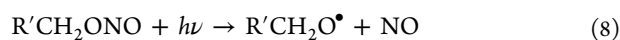


In the gas phase this process is highly efficient, with a quantum yield approaching unity for the  $\text{C}_3$ – $\text{C}_5$  alkyl nitrates ( $\lambda = 308 \text{ nm}$ ).<sup>16</sup> In the free troposphere, the alkoxy radical formed in (5) is likely to react with oxygen, yielding an aldehyde or ketone along with the hydroperoxy radical.<sup>54</sup> However, in the condensed phase under ultrahigh vacuum, this reaction with oxygen is unlikely to be important.

Upon photolysis of ethyl nitrate, significant yields of ethyl nitrite have been reported by both Rebbert<sup>7</sup> and Zhu et al.<sup>15</sup> Though Rebbert suggested that the alkyl nitrite was formed as a primary product during photolysis, Zhu et al. have produced evidence to the contrary. Through the use of cavity ring down spectroscopy, the authors demonstrated that the alkyl nitrite was formed via the secondary reactions:<sup>15</sup>



The intermediate formation of alkyl nitrites via reactions 5–7 provides a plausible explanation for the apparent generation of nitrous oxide during the photolysis of the alkyl nitrates, as evidenced by both RAIR and TPD spectra obtained in the current study. Notably, the low temperature photolysis of primary and tertiary alkyl nitrites codeposited with water yields an identical RAIR feature at 2230  $\text{cm}^{-1}$ , which begins to grow immediately upon irradiation.<sup>39</sup> In the gas,<sup>53–58</sup> matrix isolated,<sup>59–61</sup> and solid phase,<sup>39</sup> photolysis of alkyl nitrites initially leads to the formation of an aldehyde or ketone, along with the nitroxyl molecule, HNO:



Nitroxyl, formed via reaction 9, may then condense to yield nitrous oxide and water. This process is known to proceed

efficiently in the gas,<sup>55,56</sup> liquid,<sup>62,63</sup> and matrix-isolated phases:<sup>59,61</sup>



Accordingly, if the photolysis of the parent alkyl nitrate results in the formation of the corresponding alkyl nitrite, reactions 8–10 will result in the formation of nitrous oxide. Alkyl nitrites were not observed directly in the RAIR spectra of the photolyzed alkyl nitrate thin films; this is likely a result of their known photolability.<sup>54,57</sup>

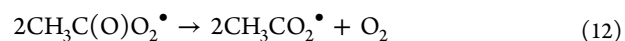
**Peroxyacetyl Nitrate (PAN).** As a result of its low symmetry ( $C_1$ ), the IR spectrum of PAN is rich in detail as all 27 normal mode vibrations of this species are IR active.<sup>47</sup> During the current RAIR investigation, the IR absorption intensities of bands attributable to PAN were found to be indistinguishable from those previously reported for the gas<sup>47,64</sup> and matrix-isolated phases,<sup>47,65,66</sup> which is accounted for by the molecular asymmetry of PAN.

Relative to gas-phase and matrix-isolated IR spectra,<sup>47,64</sup> differences in the carbonyl stretching frequency and band shape were observed during the current investigation. When deposited neat to the gold substrate, the absorption frequency of this mode is observed to be centered at 1812  $\text{cm}^{-1}$  and is red-shifted by  $\Delta\tilde{\nu} = -30 \text{ cm}^{-1}$  relative to the gas phase.<sup>47</sup> A shoulder at 1826  $\text{cm}^{-1}$  is also present in the spectrum of the neatly deposited PAN and becomes more pronounced upon codeposition with water. Although the latter peak at 1826  $\text{cm}^{-1}$  is similar to that found in the Raman spectrum of the pure liquid,<sup>47</sup> the red-shifting of the carbonyl peak to 1812  $\text{cm}^{-1}$  suggests that in the solid phase, the carbonyl group may be influenced by intermolecular interactions between neighboring PAN molecules.

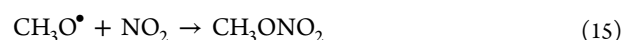
Upon photolysis of PAN, RAIR spectral features attributable to the formation of carbon dioxide and methyl nitrate were observed to develop (Figure 10). The formation of the latter was further suggested through the observation of a peak with  $m/z = 29$  in the TPD spectra which is likely due to the  $\text{CHO}^+$  fragment of methyl nitrate (Figure 12). By analogy to known thermal decomposition pathways of PAN in the gas phase,<sup>47,67</sup> the formation of methyl nitrate could result from secondary reactions of the peroxyacetyl radical formed via



Following the formation of the peroxyacetyl radical, this species may then undergo disproportionation, yielding the acetoxy radical:<sup>47</sup>



The methyl nitrate end product, together with carbon dioxide, may then be formed via<sup>68</sup>



Although reactions 13–15 were initially proposed to occur during the gas-phase thermal decomposition of PAN,<sup>47,67</sup> the production of  $\text{CO}_2$  and methyl nitrate has also been previously shown to occur during the UV photolysis of PAN trapped within Ar matrices.<sup>47</sup> This, along with evidence from the current study, suggests that such a pathway is a viable route to the observed end-products.

## CONCLUSIONS

The alkyl and peroxyacyl nitrates are both important reservoir species of  $\text{NO}_x$  in the troposphere. Owing to their relative stabilities, these species allow for the long-range transport of nitrogen oxides away from urbanized point sources, to the “pristine” polar cryosphere, where they can accumulate during the dark winter months. Although the gas-phase reactivities of these species have been well established, the potential for heterogeneous transformations of these species in frozen environments is poorly understood. Accordingly, the major low temperature loss process for alkyl and peroxyacyl nitrates in the gas phase, i.e., photolysis, was examined under laboratory conditions when these species are present within thin film mimics of environmental ices.

When codeposited with water at low temperatures ( $T = 113$  K), the alkyl nitrates investigated ( $R = \text{Me}$ ,  $i\text{-Pr}$ , and  $i\text{-Bu}$ ) were found to undergo photolysis to form aldehydes or ketones and nitrous oxide as end products. The relative loss rates of the three alkyl nitrates investigated were found to mimic those in the gas phase, which increase in the order  $R = \text{Me} < i\text{-Pr} < i\text{-Bu}$ . The formation of nitrous oxide as the major nitrogenous photoproduct was rationalized by invoking the intermediacy of the corresponding alkyl nitrites, generated as secondary products during the photolysis of the alkyl nitrates. By analogy to previous investigations, the nitrous oxide end product was shown likely to result from the dimerization of the nitroxyl molecule,  $\text{HNO}$ .

Although the  $\text{N}_2\text{O}$  product observed here is stable in the troposphere (and therefore not thought of as an  $\text{NO}_y$  species in the lower atmosphere),<sup>69</sup> the vast majority of  $\text{NO}_x$  in the stratosphere originates from the dissociation of this long-lived gas. Accordingly, in addition to its recognized role as a greenhouse gas in the troposphere,  $\text{N}_2\text{O}$  plays a crucial role in stratospheric ozone chemistry. Indeed, as shown by Ravishankara et al.,  $\text{N}_2\text{O}$  is predicted to destroy more stratospheric ozone than any other reactive chemical family during the 21st century.<sup>70</sup>

Upon exposure to UV light, the production of methyl nitrate and carbon dioxide was observed to take place within thin films of PAN codeposited with water ice. As the absorption cross sections of PAN are known to increase with increasing temperature,<sup>4</sup> this process is likely to be even more favorable under environmental temperatures compared with those used in the current study. Hence, in the upper troposphere ( $T \approx 188\text{--}228$  K) or at the poles ( $T \approx 190\text{--}273$  K)<sup>71,72</sup> photolytic decomposition of PAN adsorbed to cold surfaces via the chemistry outlined above may arise via the pathways outlined.

## AUTHOR INFORMATION

### Corresponding Authors

\*D. O'Sullivan. E-mail: d.osullivan@leeds.ac.uk.

\*R. P. McLaughlin. E-mail: mclaughlinr@seattleu.edu.

\*J. R. Sodeau. E-mail: j.sodeau@ucc.ie.

### Present Address

<sup>§</sup>School of Earth and Environment, University of Leeds, Woodhouse Lane, Leeds LS2 9JT, U.K.

### Notes

The authors declare no competing financial interest.

## ACKNOWLEDGMENTS

D.O.S. acknowledges IRCSET and SFI-RFP for their support. R.P.M. acknowledges the Fulbright Program, Council for the

International Exchange of Scholars and the Fulbright Commission in Ireland.

## REFERENCES

- (1) Jenkin, M. E.; Clemitshaw, K. C. Ozone and Other Secondary Photochemical Pollutants: Chemical Processes Governing Their Formation in the Planetary Boundary Layer. *Atmos. Environ.* **2000**, *34*, 2499–2527.
- (2) Clemitshaw, K. C.; Williams, J.; Rattigan, O. V.; Shallcross, D. E.; Law, K. S.; Anthony Cox, R. Gas-Phase Ultraviolet Absorption Cross-Sections and Atmospheric Lifetimes of Several C2-C5 Alkyl Nitrates. *J. Photochem. Photobiol. Chem.* **1997**, *102*, 117–126.
- (3) Talukdar, R. K.; Burkholder, J. B.; Hunter, M.; Gilles, M. K.; Roberts, J. M.; Ravishankara, A. R. Atmospheric Fate of Several Alkyl Nitrates Part 2 UV Absorption Cross-Sections and Photodissociation Quantum Yields. *J. Chem. Soc., Faraday Trans.* **1997**, *93*, 2797–2805.
- (4) Talukdar, R. K.; Burkholder, J. B.; Schmoltner, A.-M.; Roberts, J. M.; Wilson, R. R.; Ravishankara, A. R. Investigation of the Loss Processes for Peroxyacetyl Nitrate in the Atmosphere: UV Photolysis and Reaction with OH. *J. Geophys. Res.* **1995**, *100*, 14163–14173.
- (5) Roberts, J. M. The Atmospheric Chemistry of Organic Nitrates. *Atmos. Environ.* **1990**, *24A*, 243–287.
- (6) Roberts, J. M.; Fajer, R. W. UV Absorption Cross Sections of Organic Nitrates of Potential Atmospheric Importance and Estimation of Atmospheric Lifetimes. *Environ. Sci. Technol.* **1989**, *23*, 945–951.
- (7) Rebertus, R. E. Primary Processes in the Photolysis of Ethyl Nitrate. *J. Phys. Chem.* **1963**, *67*, 1923–1925.
- (8) Carbajo, P. G.; Orr-Ewing, A. J.  $\text{NO}_2$  Quantum Yields from Ultraviolet Photodissociation of Methyl and Isopropyl Nitrate. *Phys. Chem. Chem. Phys.* **2010**, *12*, 6084–6091.
- (9) Muthuramu, K.; Shepson, P.; Bottenheim, J.; Jobson, B.; Niki, H.; Anlauf, K. Relationships between Organic Nitrates and Surface Ozone Destruction During Polar Sunrise Experiment 1992. *J. Geophys. Res.* **1994**, *99*, 25369–25378.
- (10) Bottenheim, J. W.; Barrie, L. A.; Atlas, E. The Partitioning of Nitrogen Oxides in the Lower Arctic Troposphere During Spring 1988. *J. Atmos. Chem.* **1993**, *17*, 15–27.
- (11) Jones, A. E.; Weller, R.; Minikin, A.; Wolff, E. W.; Sturges, W. T.; McIntyre, H. P.; Leonard, S. R.; Schrems, O.; Bauguitte, S. Oxidized Nitrogen Chemistry and Speciation in the Antarctic Troposphere. *J. Geophys. Res.* **1999**, *104*, 21355–21366.
- (12) Jones, A. E.; et al. The Multi-Seasonal  $\text{NO}_y$  Budget in Coastal Antarctica and Its Link with Surface Snow and Ice Core Nitrate: Results from the Chablis Campaign. *Atmos. Chem. Phys.* **2011**, *11*, 9271–9285.
- (13) Luke, W.; Dickerson, R. Direct Measurements of the Photolysis Rate Coefficient of Ethyl Nitrate. *Geophys. Res. Lett.* **1988**, *15*, 1181–1184.
- (14) Luke, W.; Dickerson, R. R.; Nunnermacker, L. J. Direct Measurements of the Photolysis Rate Coefficients and Henry's Law Constants of Several Alkyl Nitrates. *J. Geophys. Res.* **1989**, *94 D*, 14905–14921.
- (15) Zhu, L.; Ding, C.-F. Temperature Dependence of the near UV Absorption Spectra and Photolysis Products of Ethyl Nitrate. *Chem. Phys. Lett.* **1997**, *265*, 177–184.
- (16) Zhu, L.; Kellis, D. Temperature Dependence of the UV Absorption Cross Sections and Photodissociation Products of C3-C5 Nitrates. *Chem. Phys. Lett.* **1997**, *278*, 41–48.
- (17) Csizmadia, V. M.; Houlden, S. A.; Koves, G. J.; Boggs, J. M.; Csizmadia, I. G. Stereochemistry and Ultraviolet Spectra of Simple Nitrate Esters. *J. Org. Chem.* **1973**, *38*, 2281–2287.
- (18) Orlando, J. J.; Tyndall, G. S.; Calvert, J. G. Thermal Decomposition Pathways for Peroxyacetyl Nitrate (PAN): Implications for Atmospheric Methyl Nitrate Levels. *Atmos. Environ. A: Gen. Top.* **1992**, *26*, 3111–3118.
- (19) Bridier, I.; Caralp, F.; Loirat, H.; Lesclaux, R.; Veyret, B.; Becker, K.; Reimer, A.; Zabel, F. Kinetic and Theoretical Studies of the Reactions  $\text{CH}_3\text{C}(\text{O})\text{O}_2 + \text{NO}_2 + \text{M} \leftrightarrow \text{CH}_3\text{C}(\text{O})\text{O}_2(\text{NO}_2) + \text{M}$

between 248 and 393 K and between 30 and 760 Torr. *J. Phys. Chem.* **1991**, *95*, 3594–3600.

(20) Senum, G. I.; Fajer, R.; Gaffney, J. S. Fourier Transform Infrared Spectroscopic Study of the Thermal Stability of Peroxyacetyl Nitrate. *J. Phys. Chem.* **1986**, *90*, 152–156.

(21) Roberts, J. M.; Bertman, S. B. The Thermal Decomposition of Peroxyacetic Nitric Anhydride (PAN) and Peroxymethacrylic Nitric Anhydride (MPAN). *Int. J. Chem. Kinet.* **1992**, *24*, 297–307.

(22) Kleindienst, T. Recent Developments in the Chemistry and Biology of Peroxyacetyl Nitrate. *Res. Chem. Intermed.* **1994**, *20*, 335–384.

(23) Flowers, B. A.; Angerhofer, M. E.; Simpson, W. R.; Nakayama, T.; Matsumi, Y. Nitrate Radical Quantum Yield from Peroxyacetyl Nitrate Photolysis. *J. Phys. Chem. A* **2005**, *109*, 2552–2558.

(24) Flowers, B. A.; Stanton, J. F.; Simpson, W. R. Wavelength Dependence of Nitrate Radical Quantum Yield from Peroxyacetyl Nitrate Photolysis: Experimental and Theoretical Studies. *J. Phys. Chem. A* **2007**, *111*, 11602–11607.

(25) Mazely, T. L.; Friedl, R. R.; Sander, S. P. Production of NO<sub>2</sub> from Photolysis of Peroxyacetyl Nitrate. *J. Phys. Chem.* **1995**, *99*, 8162–8169.

(26) Mazely, T. L.; Friedl, R. R.; Sander, S. P. Quantum Yield of NO<sub>3</sub> from Peroxyacetyl Nitrate Photolysis. *J. Phys. Chem. A* **1997**, *101*, 7090–7097.

(27) Harwood, M. H.; Roberts, J. M.; Frost, G. J.; Ravishankara, A. R.; Burkholder, J. B. Photochemical Studies of CH<sub>3</sub>C(O)OONO<sub>2</sub> (PAN) and CH<sub>3</sub>CH<sub>2</sub>C(O)OONO<sub>2</sub> (PPN): NO<sub>3</sub> Quantum Yields. *J. Phys. Chem. A* **2003**, *107*, 1148–1154.

(28) Senum, G.; Lee, Y.; Gaffney, J. Ultraviolet Absorption Spectrum of Peroxyacetyl Nitrate and Peroxypropionyl Nitrate. *J. Phys. Chem.* **1984**, *88*, 1269–1270.

(29) Bottenheim, J.; Gallant, A.; Brice, K. Measurements of NO<sub>y</sub> Species and O<sub>3</sub> at 82 N Latitude. *Geophys. Res. Lett.* **1986**, *13*, 113–116.

(30) Jaffe, D. In *The Tropospheric Chemistry of Ozone in the Polar Regions*; Niki, H., Becker, K. H., Eds.; Springer Verlag: Berlin, 1993; p 105.

(31) Horn, A. B.; Koch, T.; Chesters, M. A.; McCoustra, M. R. S.; Sodeau, J. R. A Low-Temperature Infrared Study of the Reactions of the Stratospheric NO<sub>y</sub> Reservoir Species Dinitrogen Pentoxide with Water Ice, 80–160 K. *J. Phys. Chem.* **1994**, *98*, 946–951.

(32) Koch, T. G.; Holmes, N. S.; Roddis, T. B.; Sodeau, J. R. Low-Temperature Reflection/Absorption IR Study of Thin Films of Nitric Acid Hydrates and Ammonium Nitrate Adsorbed on Gold Foil. *J. Chem. Soc., Faraday Trans.* **1996**, *92*, 4787–4792.

(33) Nikitas, C.; Clemmshaw, K.; Oram, D.; Penkett, S. Measurement of PAN in the Polluted Boundary Layer and Free Troposphere Using a Luminol-NO<sub>2</sub> Detector Combined with a Thermal Converter. *J. Atmos. Chem.* **1997**, *28*, 339–359.

(34) Brand, J. C. D.; Cawthon, T. M. The Vibrational Spectrum of Methyl Nitrate. *J. Am. Chem. Soc.* **1955**, *77*, 319–323.

(35) Lannon, J. A.; Harris, L. E.; Verderame, F. D.; Thomas, W. G.; Lucia, E. A.; Koniers, S. Infrared Spectra and Intermolecular Potentials of Matrix Isolated Methyl Nitrate and Methyl-D<sub>3</sub>-Nitrate. *J. Mol. Spectrosc.* **1974**, *50*, 68–81.

(36) Hollas, J. M. *Modern Spectroscopy*, 4th ed.; Wiley: Chichester, U.K., 1993; p 157.

(37) Khoshkoo, H.; Hemple, S.; Nixon, E. Infrared and Raman Studies of Solid Formaldehyde. *Spectrochim. Acta A* **1974**, *30*, 863–868.

(38) Hellebust, S.; Roddis, T.; Sodeau, J. Potential Role of the Nitroacidium Ion on HONO Emissions from the Snowpack. *J. Phys. Chem. A* **2007**, *111*, 1167–1171.

(39) McLaughlin, R. P.; O'Sullivan, D.; Sodeau, J. R. Cold-Surface Photochemistry of Primary and Tertiary Alkyl Nitrites. *J. Phys. Chem. A* **2012**, *116*, 6759–6770.

(40) McLaughlin, R. P.; Bird, B.; Reid, P. J. Vibrational Analysis of Isopropyl Nitrate and Isobutyl Nitrate. *Spectrochim. Acta A* **2002**, *58*, 2571–2580.

(41) Schaff, J. E.; Roberts, J. T. The Adsorption of Acetone on Thin Films of Amorphous and Crystalline Ice. *Langmuir* **1998**, *14*, 1478–1486.

(42) Koch, T. G.; Sodeau, J. R. Photochemistry of Dinitrogen Pentoxide in Low-Temperature Matrices. *J. Chem. Soc., Faraday Trans.* **1996**, *92*, 2347–2351.

(43) Brenninkmeijer, C.; Röckmann, T. Mass Spectrometry of the Intramolecular Nitrogen Isotope Distribution of Environmental Nitrous Oxide Using Fragment-Ion Analysis. *Rapid Commun. Mass Spectrom.* **1999**, *13*, 2028–2033.

(44) Gálvez, Ó.; Ortega, I. K.; Maté, B.; Moreno, M. Á.; Martín-Llorente, B.; Herrero, V. J.; Escibano, R.; Gutiérrez, P. J. A Study of the Interaction of CO<sub>2</sub> with Water Ice. *Astron. and Astro.* **2013**, *472*, 691–698.

(45) Smith, R. S.; Huang, C.; Wong, E. K. L.; Kay, B. D. The Molecular Volcano: Abrupt CCl<sub>4</sub> Desorption Driven by the Crystallization of Amorphous Solid Water. *Phys. Rev. Lett.* **1997**, *79*, 909–917.

(46) Durig, J. R.; Guirgis, G. A.; Brewer, W. E.; Little, T. S. Vibrational Spectra and Structure, Ab Initio Calculations, and Conformational Stability of 2-Methylpropanal. *J. Mol. Struct.* **1991**, *248*, 49–77.

(47) Bruckmann, P. W.; Willner, H. Infrared Spectroscopic Study of Peroxyacetyl Nitrate (PAN) and Its Decomposition Products. *Environ. Sci. Technol.* **1983**, *17*, 352–357.

(48) Fraser, R. T. M.; Paul, N. C. The Mass Spectrometry of Nitrate Esters and Related Compounds. Part I. *J. Chem. Soc. B: Phys. Org.* **1968**, 659–663.

(49) Louw, R.; Sluis, G.; Vermeeren, H. Facile Preparation of Peroxyacetyl Nitrates. *J. Am. Chem. Soc.* **1975**, *97*, 4396–4397.

(50) Takagi, H.; Washida, N.; Akimoto, H.; Okuda, M. Analysis of Nitrate and Nitrite Esters by Gas Chromatography/Photoionization Mass Spectrometry. *Anal. Chem.* **1981**, *53*, 175–179.

(51) Jenniskens, P.; Banham, S. F.; Blake, D. F.; McCoustra, M. R. Liquid Water in the Domain of Cubic Crystalline Ice Ic. *J. Chem. Phys.* **1997**, *107*, 1232–1241.

(52) Urbanski, T.; Witanowski, M. Infra-Red Spectra of Nitric Esters. Part 1. Influence of Inductive Effects of Substituents. *Trans. Faraday Soc.* **1963**, *59*, 1039–1045.

(53) Horn, A. B.; Banham, S. F.; McCoustra, M. R. S. Optical Effects in the IR Reflection-Absorption Spectra of Thin Water-Ice Films on Metal Substrates. *J. Chem. Soc., Faraday Trans.* **1995**, *91*, 4005–4008.

(54) Finlayson-Pitts, B.; Pitts, J. *Chemistry of the Upper and Lower Atmosphere Theory, Experiments, and Applications*; Academic Press: San Diego, CA, 2000; p 221.

(55) Wiebe, H. A.; Hecklen, J. Photolysis of Methyl Nitrite. *J. Am. Chem. Soc.* **1973**, *95*, 1–7.

(56) Napier, I.; Norrish, R. The Photolysis and Pyrolysis of Nitromethane and Methyl Nitrite. *Proc. R. Soc. London, Ser. A* **1967**, *317*–336.

(57) Calvert, J.; Pitts, J. *Photochemistry*; Wiley: New York, 1966; p 362.

(58) Hanst, P. L.; Calvert, J. G. On the Mechanism of Ozone Production in the Photo-Oxidation of Alkyl Nitrites. *J. Phys. Chem.* **1959**, *63*, 2071–2073.

(59) Brown, H.; Pimentel, G. Photolysis of Nitromethane and of Methyl Nitrite in an Argon Matrix; Infrared Detection of Nitroxyl, HNO. *J. Chem. Phys.* **1958**, *29*, 883–890.

(60) Jacox, M. E.; Rook, F. L. Photodecomposition of Methyl Nitrite Trapped in Solid Argon. *J. Phys. Chem.* **1982**, *86*, 2899–2904.

(61) Mátyus, E.; Magyarfalvi, G.; Tarczay, G. Conformers and Photochemistry of Propyl Nitrites: A Matrix Isolation Study. *J. Phys. Chem. A* **2006**, *111*, 450–459.

(62) Fukuto, J. M.; Bartberger, M. D.; Dutton, A. S.; Paolucci, N.; Wink, D. A.; Houk, K. N. The Physiological Chemistry and Biological Activity of Nitroxyl (HNO): The Neglected, Misunderstood, and Enigmatic Nitrogen Oxide. *Chem. Res. Toxicol.* **2005**, *18*, 790–801.

- (63) Fukuto, J. M.; Switzer, C. H.; Miranda, K. M.; Wink, D. A. Nitroxyl (HNO): Chemistry, Biochemistry, and Pharmacology. *Annu. Rev. Pharmacol. Toxicol.* **2005**, *45*, 335–355.
- (64) Fild, I.; Lovell, D. J. Infrared Spectral Studies of Peroxyacetyl Nitrate (PAN). *J. Opt. Soc. Am.* **1970**, *60*, 1315–1318.
- (65) Adamson, P.; Günthard, H. H. Reinvestigation of the Matrix I.R. Spectrum of Peroxyacetylnitrate (PAN). *Spectrochem. Acta A* **1980**, *36*, 473–475.
- (66) Varetti, E.; Pimentel, G. The Infrared Spectrum of <sup>15</sup>N-Labeled Peroxyacetylnitrate (PAN) in an Oxygen Matrix. *Spectrochem. Acta A* **1974**, *30*, 1069–1072.
- (67) Cox, R. A.; Roffey, M. J. Thermal Decomposition of Peroxyacetylnitrate in the Presence of Nitric Oxide. *Environ. Sci. Technol.* **1977**, *11*, 900–906.
- (68) Atkinson, R.; Baulch, D. L.; Cox, R. A.; Hampson, R. F.; Kerr, J. A. Evaluated Kinetic and Photochemical Data for Atmospheric Chemistry, Supplement Iv. *J. Phys. Chem. Ref. Data* **1992**, *21*, 1125.
- (69) Wayne, R. P. *Chemistry of Atmospheres*, 3rd ed.; Oxford University Press: New York, 2000; p 166.
- (70) Ravishankara, A.; Daniel, J. S.; Portmann, R. W. Nitrous Oxide (N<sub>2</sub>O): The Dominant Ozone-Depleting Substance Emitted in the 21st Century. *Science* **2009**, *326*, 123–125.
- (71) Siegert, M. J. Lakes beneath the Ice Sheet: The Occurrence, Analysis, and Future Exploration of Lake Vostok and Other Antarctic Subglacial Lakes. *Annu. Rev. Earth Planet. Sci.* **2005**, *33*, 215–245.
- (72) McBean, G.; et al. Arctic Climate: Past and Present, *Arctic Climate Impact Assessment*; Cambridge University Press: Cambridge, U.K., 2005; pp 21–60.